Pharmacological Modulation of Neurite Outgrowth in Human Neural Progenitor Cells by Inhibiting Non-Muscle Myosin II

Julianna Lilienberg
Research Centre for Natural Sciences Institute of Enzymology: Termeszettudomanyi Kutatokozpont Enzimologiai Intezet

Zoltán Hegyi
Research Centre for Natural Sciences Institute of Enzymology: Termeszettudomanyi Kutatokozpont Enzimologiai Intezet

Eszter Szabó
Research Centre for Natural Sciences Institute of Enzymology: Termeszettudomanyi Kutatokozpont Enzimologiai Intezet

Edit Hathy
Semmelweis University: Semmelweis Egyetem

András Málnási-Csizmadia
Eötvös Loránd Tudományegyetem: Eotvos Lorand Tudomanyegyetem

János M. Réthelyi
Semmelweis University: Semmelweis Egyetem

Ágota Apáti
Research Centre for Natural Sciences Institute of Enzymology: Termeszettudomanyi Kutatokozpont Enzimologiai Intezet

László Homolya (homolya.laszlo@ttk.hu)
Research Centre for Natural Sciences Institute of Enzymology: Termeszettudomanyi Kutatokozpont Enzimologiai Intezet https://orcid.org/0000-0003-1639-8140

Research article

Keywords: human neural progenitor cells, blebbistatin, neurite, non-muscle myosin II, extracellular matrix

Posted Date: April 28th, 2021

DOI: https://doi.org/10.21203/rs.3.rs-443732/v1

Abstract

Studies on neural development and neuronal regeneration are mainly based on animal models. The establishment of pluripotent stem cell technology, however, opened new perspectives for better understanding these processes in humans by providing unlimited cell source for hard-to-obtain human tissues. Here, we aimed at identifying the molecular factors that confine and modulate an early step of neural regeneration, the formation of neurites in human neural progenitor cells (NPCs). eGFP was stably expressed in NPCs differentiated from human embryonic and induced pluripotent stem cell lines, and the neurite outgrowth was investigated under permissive and restrictive conditions using a high-content screening system. We found that the non-muscle myosin II (NMII) inhibitor blebbistatin and its novel, non-toxic derivatives initiate extensive neurite outgrowth in human NPCs. We observed that the extracellular matrix components greatly influence the rate of neurite formation, but NMII inhibitors are able to override the inhibitory effect of the restrictive environment. Similar, non-additive stimulatory effect on neurite generation was detected by the inhibition of ROCK1 kinase, the upstream regulator of NMII, whereas inhibition of JNKs had negligible effect, suggesting that ROCK1 signal is dominantly manifested by the actomyosin activity. In addition to providing a reliable cell-based *in vitro* model for identifying intrinsic mechanisms and environmental factors responsible for impeded axonal regeneration in humans, our results demonstrate that NMII and ROCK1 are important pharmacological targets for the augmentation of neural regeneration at the progenitor level, and may open novel perspectives in to development of more effective pharmacological and cell therapies for various neurodegenerative disorders.

Background

Neurodegenerative disease conditions, such as Huntington's disease, Alzheimer's disease, and Parkinson's disease are characterized by progressive loss of various types of neurons. Regenerative mechanisms, which are fairly limited in adult neural tissue, may delay or even stall disease progression. A major determinant of the hindered neuronal regeneration is the diminished axonal growth capacity of mature neurons. Extensive studies have been performed to elucidate the process of axonal growth impairment (1–19), and revealed the importance of environmental inhibitory mechanisms in addition to the intrinsic factors of retarded axonal growth (2, 20–24). Because of the limited availability of human neural tissues, most of these studies used rodent or avian models.

Introduction of human pluripotent stem cells (PSCs) opens a new perspective for neurobiological research. Although application of stem cells obtained from early embryos raises several ethical issues, employing induced pluripotent stem cells (iPSCs) reprogrammed from adult tissues dispels these concerns. Differentiation of either embryonic stem cells (ESCs) or iPSCs into NPCs and subsequently into mature neurons makes possible the *in vitro* investigation of human neural development and regeneration, as well as allows us to study the pharmacological modulation of neural cells of human origin.

Human neural progenitor cells, which represent *in vivo* a reservoir for neural regeneration, can be generated from human pluripotent stem cells by directed differentiation. These cells resemble the usual

cell lines in several aspects, as they can be passaged numerous times, cryopreserved, and transfected with various transgenes. At basal state, NPCs have a low number of short processes (1–2 per cell) with no substantial branching. However, when they start to differentiate into neurons, as an initial step, NPCs protrude projections, which subsequently elongate and branch. Later one of the projections differentiates into the extended axon, while the others become dendrites.

Neurite outgrowth is a dynamic process; the elongation of these protrusions is not unidirectional but a result of recurrent growth and retrieval. At the tip of these projections, actin dynamics, which is driven by numerous factors, has a crucial role. One of these factors is the non-muscle myosin II, which is an ATP-driven molecular motor protein responsible for the retrograde actin flow (recently reviewed in (25)). Blebbistatin (BS) is a well-characterized, selective and potent inhibitor of NMII (26), which blocks myosin heads in a low affinity state for actin, thus preventing formation of actomyosin complexes (27, 28). Despite BS being widely used in studies on actomyosin network function it holds a number of unfavorable properties, such as poor water-solubility, stability issues, fluorescence interference, cytotoxicity and even phototoxicity (29). To overcome these negative properties of blebbistatin several BS-derivatives have recently been developed. The most promising derivatives, which are non-fluorescent, highly soluble and non-toxic compounds, include para-nitroblebbistatin (NBS) and para-aminoblebbistatin (AmBS) (30–33).

In the present work, we have generated human stem cell-derived NPCs expressing enhanced green fluorescent protein (eGFP-NPC) at high level, and studied the neurite outgrowth using high-content fluorescence microscopy. We examined how various components of the extracellular matrix (ECM) influence the protrusion of neurites, and the effect of BS and its derivatives on neurite outgrowth in permissive and inhibitory environments. We found that BS and its derivatives stimulate profound neurite outgrowth in human NPCs, and can abrogate the inhibitory effect of most detrimental ECM components. Contrary to primary cells isolated from rodent or avian embryos, the applied cellular model system, i.e., the human stem cell-derived NPCs, has the benefit of providing information on the molecular mechanisms of neuronal regeneration relevant to humans, and can help to develop new therapeutic approaches to ameliorate nervous system injuries.

Materials And Methods

Generation of pluripotent stem cell-derived NPCs expressing eGFP

A human iPSC line, previously generated from fibroblasts of a healthy male individual by Sendai virus reprogramming (34), was kindly provided by Fred H. Gage (Salk Institute), whereas the human ESC line, HUES9 was a kind gift from Douglas A. Melton (Howard Hughes Medical Institute). These cell lines were differentiated into NPCs by a directed differentiation protocol, which is based on a previously published, multistep procedure (35), and somewhat modified in our laboratory (Suppl. Figure 1). Briefly, PSCs were cultured in mTeSR media (Stem Cell Technologies) on Matrigel-coated dishes (Corning), and passaged by

ReLSR (Invitrogen). Embryoid bodies (EBs) were generated from human PSCs on low-adherence plates; then the cells were differentiated toward the neural lineage using DKK1 (PeproTech), SB431542 (Sigma), Noggin (Thermo Fisher Scientific), and cyclopamine (Sigma). After 21 days, the EBs were seeded onto plates previously coated with poly-ornithine/laminin (Sigma and Thermo Fisher Scientific), then cultured for an additional 7 days. Appearing rosettes were collected and dissociated, and then the cells were plated onto plates previously coated with poly-ornithine and laminin (see below). When attached NPCs became super-confluent, they were transferred onto new poly-ornithine/laminin-coated plates.

To obtain stable expression of eGFP in human NPCs, a Sleeping Beauty transposon-based gene delivery method was applied (36). NPCs were co-transfected with a plasmid harboring a CAG promoter-driven eGFP and puromycin resistance gene (Suppl. Figure 2a, left panel), as well as with another vector containing CMV promoter-driven Sleeping Beauty transposase. Transfection was carried out using Fugene HD reagent (Thermo Fisher Scientific) according to the manufacturer's instructions. Eight days following transfection, the cells were subjected to 1.6 µg/ml puromycin for 24 hours. To obtain cell populations expressing different levels of eGFP, the cells were sorted by a FACS Aria cell sorter (Suppl. Figure 2a, middle and right panels).

Surface coating and cell culturing

Six-well plates (Greiner) were coated with 2 ml of 10 µg/ml poly-ornithine solution for 24 hours at RT. The wells were then washed three times with phosphate-buffered saline (PBS, Thermo Fisher Scientific), and 2 ml of 5 µg/ml laminin solution was added for an additional 16 hours at 4°C. $3\text{-}5{\cdot}10^5$ NPCs were seeded into each well, and cultured in DMEM/F-12, Glutamax™ medium supplemented with N2 Supplement-A, B27 (all from Thermo Fisher Scientific), basic fibroblast growth factor (Invitrogen), Antibiotic-Antimycotic (Gibco) and laminin (1 µg/ml). The culture medium was replaced every other day. Confluent wells were washed with PBS, and the cells were detached with a 5-minute Accutase (Stem Cell Technologies) treatment.

For experiments, 96-well plates (Greiner) were coated with various extracellular matrices as follows: Matrigel, previously thawed on ice and dissolved in cold media (50 µg/ml), was distributed into pre-chilled 96-well plates (100 µl per well), which were then incubated for 24 hours at 4°C. Alternatively, the plates were treated with 100 µl of poly-ornithine (10 µg/ml) or poly-lysine (100 µg/ml, Sigma) for 24 hours at RT, followed by overlaying with 200 µl laminin (5 µg/ml), where indicated. Other surface treatments included coating with 100 µl of aggrecan (Aggr, 50 µg/ml, Sigma), chondroitin sulfate (CS, 10 µg/ml, Merck), myelin oligodendrocyte glycoprotein (MOG, 50 µg/ml, Sigma) and chondroitin-sulfate proteoglycan (CSPG, 10 µg/ml, Merck) solutions for 24 hours at 4°C.

Neurite outgrowth measurements and analysis

$3\text{-}5{\cdot}10^3$ NPCs expressing eGFP at a high level (eGFP-NPCs) were seeded onto a 96-well plate previously coated with various ECM components. After 2 hours, the cells were subjected to NMII, ROCK1, or JNK inhibitors at various concentrations, as indicated. While NBS and AmBS were produced as described

previously (33), the ROCK1-selective inhibitor Y27632 and the pan-JNK inhibitor SP600125 were purchased from Sigma. Green fluorescence images were acquired by an ImageXpress Micro XLS instrument (Molecular Devices) equipped with environment control unit providing 37°C temperature and humidified atmosphere containing 5% CO_2, 20% O_2, and 75% N_2. Six fields of view, covering approximately 40% of the total well surface, were imaged for 4 hours in 15 minutes intervals using an FITC filter cube (ex. 482/35 nm, em. 536/40 nm) and a 10x Nikon objective (Plan Fluor, NA = 0.3). All conditions were measured in three technical parallels.

For quantitative analysis, the total neurite lengths were assessed in each field of view using the Neurite Outgrowth module of MetaXpress software (Molecular Devices). The maximum width for cell bodies was defined as 150 μm not to exclude tight groups of cells from the analysis. The minimum fluorescence intensity of cell bodies was set to 3000 arbitrary units (AU) over the background on the 16-bit images (dynamic range 0-65535). The criterion parameters for neurites were as follows: maximum width 10 μm, minimum fluorescence intensity 500 AU, and minimum extension from the cell body 20 μm. For all analyses, the total neurite lengths were determined. To eliminate errors originating from initial cell number variations, the kinetic curves were normalized to initial cell numbers, and background was subtracted. To analyze the initial neurite growth rates, the first 3 points of the kinetic curves, encompassing a 30-minute period, were linearly fitted, and slopes were used as an output parameter. For statistical analyses, unpaired, 2-tailed, Student's t-tests were used. The results are expressed as mean ± S.E.M obtained from at least three independent experiments.

Results

Stimulation of neurite outgrowth in human NPCs by blebbistatin and its derivatives

Human fibroblast-derived iPSC and a human embryonic stem cell line, HUES9 were differentiated into NPCs. The obtained NPCs can be further differentiated into various neural cell types, especially to a population enriched in PROX1-positive dentate gyrus granule cells as we previously demonstrated (34). To assess neurite outgrowth, eGFP was stably expressed in these NPC lines using the Sleeping Beauty transposon-based gene delivery system (Suppl. Figure 2a, left panel). To obtain homogenous cell populations, following selection with puromycin (1.6 μM), the eGFP-NPCs were sorted by FACS into populations exhibiting various levels of eGFP expression (Suppl. Figure 2a, middle and right panels). Acquisition of fluorescence signals in the eGFP-NPCs, especially the ones with high eGFP expression level, resulted in high contrast images allowing visualization of thin cellular projections. Negligible phototoxic effect was observed even during long-term experiments with frequent illuminations (data not shown). We also checked whether the insertion of eGFP cDNA into the NPC genome caused any alteration in cell morphology or proliferative capacity of the NPCs, but no effect of the transgene was observed (Fig. 1a-b).

Human NPCs expressing eGFP at high levels were employed to study neurite dynamics using a high-content screening and analysis system. As detailed in the Methods section, approximately 40% of total surface area was analyzed, and even fine structures, such as neurites, with dim fluorescence were properly identified (see Suppl. Figure 2b). The cells were first seeded onto poly-ornithine/laminin-coated surface, as this coating has been proposed as an optimal condition for NPC culturing (35, 37). Two hours after seeding the cells fully adhered to the surface, and started to protrude 1–3 projections per cell (2.1 ± 0.09 as an average). The steady state length of these neurites was approximately 20 μm (17.8 ± 0.3 μm) each with negligible branching (0.055 ± 0.008 branches per neurite). These steady state values were a result of recurrent elongation and retrieval of the projections (Suppl. Video 1).

When the iPSC-derived NPCs were subjected to blebbistatin, rapid outgrowth of neurites was observed (Suppl. Video 2). As shown in Fig. 2a, BS stimulated neurite protrusion at a concentration as low as 0.25 μM, but its effect was more pronounced above 2 μM. The morphological changes observed in NPC treated with 20 μM BS may suggest toxic effect of BS at these higher concentrations, and can explain why less stimulatory effect was seen at 20 μM than at lower concentrations (5 μM and 10 μM). Less toxic and more water-soluble derivatives of BS, para-nitroblebbistatin and para-aminoblebbistatin also promoted neurite outgrowth in human NPCs (Fig. 2b-c). Contrary to BS, these derivatives were fully effective even at high concentrations. It should also be noted that AmBS appeared to be less potent than BS and NBS. The maximal stimulatory effect of AmBS was achieved only at 40 μM concentration. The cytotoxicity of BS, NBS, and AmBS was also checked, but no significant reduction in the cell numbers were observed in the given period (Fig. 1c), although a slight decrease was seen, when BS or NBS was applied at higher concentration (20 μM).

The stimulatory effect of NBS on neurite outgrowth in NPCs differentiated from HUES9 cells was similar to that seen in iPSC-derived progenitor cells (Suppl. Figure 3). The initial rate of NBS-stimulated neurite outgrowth was determined on each kinetic curve, and dose-response relationships for both HUES- and iPSC-derived NPCs were generated. No substantial differences between these two types of NPC lines were observed (Fig. 2d). The EC_{50} values for NBS stimulation in HUES- and iPSC-derived NPCs were 3.97 ± 0.34 μM and 3.11 ± 0.25 μM, respectively.

In addition to investigating the total neurite lengths in the studied fields of view and their relative change in response to BS compounds, we also analyzed alteration in cell morphology. At basal state, 2 hours after seeding, NPCs possessed ~2 neurites per cell with the total length of 30.0 ± 1.9 μm on average. After an additional 3-hour period, the number of processes remained unaltered, but the length slowly elevated to 34.4 ± 1.9 μm per cell. However, when NPCs were treated with BS, NBS, or AmBS, the neurite lengths per cell extensively increased in a dose dependent manner reaching 73.8 ± 2.4, 87.9 ± 4.1, and 94.8 ± 7.0 μm per cell, respectively (Fig. 3a), which is in concert with our previous observations shown in Fig. 2. Interestingly, the number of processes also increased close to 4 neurites per cell (Fig. 3b). In terms of neurite length, AmBS was the most efficacious, but less potent than the other two BS compound; whereas regarding number of processes, NBS was the most potent and most efficacious BS derivative. Under basal conditions, the neurites of NPCs exhibit hardly any branching: every 15th process has one

branching. BS and BS derivatives stimulated neurite branching to some extent (Fig. 3c). AmBS was the most effective in this regard: every third neurite showed branching after the treatment with 80 μM AmBS. It is noteworthy that the potency of AmBS for branching was even less than that for neurite length or process number.

Effect of extracellular matrix components on neurite outgrowth

To investigate how various extracellular matrix components influence neurite generation capability of human NPCs, the cells were seeded onto 96-well plates coated with diverse compounds. The frequently used, so-called growth-permissive extracellular matrices included Matrigel, laminin, poly-ornithine, poly-lysine, and combinations of poly-ornithine and laminin, as well as poly-lysine and laminin. Cell attachment and neurite outgrowth were substantially diminished, when human NPCs were seeded onto uncoated surface (data not shown). However, a steady basal neurite outgrowth was observed (2.51 ± 0.28 μm/min/cell two hours after plating), when NPCs were plated onto poly-ornithine/laminin-coated surface. This condition was considered as a reference point for the experiments investigating the effect of various ECMs (Fig. 4a). Similar neurite growth rates were seen in NPCs seeded on support coated with laminin alone or in combination with poly-lysine. A slight reduction was observed when the cells were grown on Matrigel, whereas poly-ornithine or poly-lysine alone provided suboptimal conditions for NPC neurite outgrowth. It is important to note that these different ECMs markedly influenced cell morphology as demonstrated in Suppl. Figure 4. On poly-ornithine/laminin or Matrigel, the NPCs attached well, spread and formed small groups of cells with several outgrowths. NPCs seeded on poly-ornithine- or poly-lysine-coated support also adhered to the surface, but exhibited round-shape and remained dispersed. Despite these observations, the cell viability was not affected by these conditions (data not shown).

Next, we examined the effects of NBS and AmBS on the neurite formation of NPCs seeded on various ECMs. To achieve maximal stimulation and to avoid the toxic effects, NBS and AmBS were applied in 10 μM and 20 μM concentrations, respectively. We found that both blebbistatin derivatives significantly promoted neurite outgrowth (approx. 3-fold) regardless of the surface coating (Fig. 4a). Since the basal neurite growth rates were smaller on poly-ornithine or poly-lysine, the stimulated ones were also less pronounced.

Several extracellular matrix components, mostly proteoglycans, produced primarily by oligodendrocytes, were proposed as potential inhibitors of neuronal regeneration (1). Therefore, in the next set of experiments, we examined the effects of Aggr, CS, MOG, and CSPG on neurite outgrowth capacity of human NPCs. When laminin was replaced with these compounds in the extracellular coat, all studied ECM components strongly inhibited neurite generation (Fig. 4b). Amongst them CSPG was the most potent. When NPCs seeded on inhibitory coatings were subjected to NBS or AmBS at the maximal effective concentration, these compounds were able to override the inhibitory effect of the ECM components. However, the stimulation of NBS did not reach the levels achieved with NPCs on the permissive coating (poly-ornithine/laminin). AmBS was even less effective; in most of the cases, its

stimulation resulted in a neurite growth rate comparable with control level, i.e., NPCs on poly-ornithine/laminin without stimulation. However, the inhibition of CSPG was so profound that either NBS, or AmBS could promote neurite outgrowth to only a small extent (Fig. 4b).

Next, we investigated the effect of laminin, which is a key component of the basal membranes and provides efficient axon guidance. In a previous experiment (Fig. 4a), we observed beneficial effect of laminin on NPC neurite outgrowth rate. When the extracellular coat contained laminin besides poly-ornithine and the inhibitory ECM components, the harmful effects of Aggr, CS, and CSPG were still significant; however, their impact was attenuated to some extent (Fig. 4c). Moreover, the inhibitory effect of MOG was reversed. Here too, NBS and AmBS were able to override the effect of inhibitory ECM components. Their stimulatory effects were comparable to the ones found in NPCs on permissive coating with only one exception. AmBS was not that effective when employed to NPCs seeded onto CSPG-containing ECM, however, its stimulatory effect was still significant (Fig. 4c).

Role of ROCK1 and JNK in neurite outgrowth in human NPCs

Next, we investigated two distinct signaling pathways, which have been reported to regulate neurite outgrowth in animal model systems. ROCK1 is an upstream regulator of NMII, and has been shown to increase actin-arc contraction and translocation rates (38). JNKs have been reported to play a key role in the stabilization and bundling of microtubules with an enhanced activity during neurite generation (39).

In the recent experiments, the human NPCs seeded onto poly-ornithine/laminin coated surface were subjected to inhibitors of ROCK1 or JNK, and the neurite outgrowth rate was assessed as described above. The ROCK1-selective inhibitor, Y27632 significantly stimulated neurite outgrowth in NPCs to an extent comparable with that the blebbistatin derivatives, NBS and AmBS elicited (Fig. 5a). In contrast, SP600125, a pan-JNK inhibitor had no effect on the neurite generation. The inhibitory potential of the compound was confirmed in an *in vitro* kinase assay (data not shown). The effect of the ROCK1 inhibitor was not additive when co-administered with either NBS or AmBS (Fig. 5b-c). The JNK inhibitor had no marked effect on NBS- or Y27632-elicited neurite outgrowth, but slightly reduced the neurite growth rate when the NPCs were stimulated with AmBS (Fig. 5b-d). Our observations suggest that NMII and ROCK1 inhibition affect the same pathway modulating neurite outgrowth in human NPCs.

In addition to neurite growth rates, the morphology changes in response to Y27632 and SP600125 have also been analyzed (Fig. 6). The ROCK1 inhibitor stimulated not only neurite length per cell, but also increased the number of processes per cell and the number of branches per neurites. In contrast, JNK inhibitor had no effect on any of these morphological parameters. Interestingly, the potency and efficacy of Y27632 was similar to NBS in terms of neurite growth and branching (Figs. 6a and c), but not for the stimulation of number of processes per cell, which parameter plateaued at around 3 (Fig. 6b).

Discussion

Neural progenitor cells represent a cell population, which plays a pivotal role in the development of nervous system during ontogeny, as well as in neural regeneration. Investigation of these processes in humans is greatly restricted due to ethical issues and the limited availability of human neural tissue, especially of the central nervous system (CNS). Most studies on neural development and regeneration are based on animal models, predominantly on primary cultures of high plasticity cells isolated from rodent (1–15) and avian (4, 16, 17) embryos and newborns. Nevertheless, NPCs differentiated from human pluripotent stem cells provide an opportunity to study neural development in human cell-based models.

Neural cells, especially neurons, exhibit a unique polar architecture. Polarization of neural cells is an essential part of neuronal differentiation, thus being fundamental in neural network formation and nerve regeneration. One of the very first episodes of neural polarization is the protrusion of a number of processes from NPCs, which event is followed by the elongation and branching of the evolving neurites. Eventually, one of the projections differentiates into the axon, whereas others develop into dendrites. A fine balance between positive and negative regulatory mechanisms, including both internal and environmental factors, ultimately leads to the establishment and maintenance of the neuronal structure. In the present study, we established an experimental instrumentation, which is suitable for studying the initial step of neural polarization, the neurite outgrowth process in NPCs of human origin. We have differentiated human pluripotent stem cells (ESCs and iPSCs) into neural progenitor cells, using a recent protocol for generation NPCs committed to the hippocampal dentate gyrus lineage (34, 35). Human neural progenitors have a key role in neurogenesis and are potential source for the stem cell-based therapies of neurodegenerative diseases. Moreover, dentate gyrus neural progenitor cells are essential for learning, pattern separation, and spatial memory formation (28); deviations of these cells can cause several disease conditions. Thus, the investigation of neurite polarization mechanism in these cell types can help to improve our strategies on neuro-regeneration and cell-based therapies. Using a transposon-based gene delivery system and cell sorting, we established high-level and stable expression of eGFP in human NPCs. We also demonstrated that eGFP expression did not affected cell growth capacity. High-content microscopy imaging and analysis of these cells allowed us to quantitate the extent and speed of neurite generation, as well as to characterize the developing neurites in term of process number per cell and branching. We found that under basal conditions, human NPCs develop only a small number (1–3) of processes, which are relatively short (30 μm) and have typically no branches (only 1 in 10 neurites).

Development of cell protrusions is complex dynamic process, which is a result of numerous events that involve not only membrane dynamics but also rearrangement of cytoskeletal elements. The structure of neurites is established by stable microtubule bundles and highly dynamic mesh of filamentous actin (F-actin). Critical steps of neurite development include the evolvement of microtubules at the positive ends, their bundling, and the continuous remodeling of actin filaments (40). The ATP-driven molecular motor protein, the non-muscle myosin binds to F-actin and controls the dynamics of actomyosin locomotion, a fundamental biological process, which is connected to numerous cellular and physiological functions including muscle contraction, cell differentiation, migration and polarization (41, 42).

Blebbistatin is a widely used, potent inhibitor of NMII (26, 27), and proved to be a useful tool for studying neuronal differentiation. Treatment of neural cells with blebbistatin results in extensive outgrowth of neurites as a consequence of abolished retrograde actin flow, when the balance of evolvement and retrieval of cell protrusion is shifted to former side. Several studies employed blebbistatin to demonstrate the role of actomyosin contractility using primary neurons from mice (1–5), rats (4–15), chickens (4, 16, 17), or even gastropods, such as *Aplysia* (18) and *Helisoma trivolvis* (19). These studies were performed in non-human primary neural cells, and investigated the neurite growth on matured neurons. The role of actomyosin in cannabinoid-induced changes in neuronal morphology was also established by blebbistatin inhibition in primary rat neurons and Neuro2a, murine neuroblastoma cells (10).

Only few studies employed human pluripotent stem cell-derived neural models to investigate the involvement of actomyosin contractility in neural polarization and differentiation. Human ESCs were treated with blebbistatin to demonstrate the role of NMII in topography-induced neuronal maturation (43). Blebbistatin antagonized differentiation of human iPSCs into midbrain dopaminergic neurons induced by mRNAs coding proneural transcription factors, also implying the involvement of NMII (44). A large-scale screening for bioactive small molecules regulating neurite growth identified blebbistatin as a hit compound (108 hits out of 4421) (45). For the high-throughput screen, iCell neurons were used, which are human iPSC-derived, cortical-like neural cultures consisting mostly of GABAergic interneurons. Contrary to the studies above, where differentiated neurons were investigated, we examined the role of NMII in human neural progenitor cells. We found that blebbistatin induces not only elongation of existing neurites but stimulates generation of new projections in human NPCs. Although branch formation of neurites was also stimulated by blebbistatin (~3-fold), it remained meager at least within the studied time frame (4 hours).

Although blebbistatin is widely used, it has numerous drawbacks when employed in cell biology applications. These include chemical instability, low solubility in water, toxicity to cells, and blue light-induced phototoxicity (29, 32). Blebbistatin also tends to form fluorescent precipitates, which interfere with many cell biology assessments. A-ring modification of blebbistatin results in higher water solubility, but comes at the cost of lower potency for NMII inhibition (46). D-ring-modified blebbistatin analogs, however, such as 3'-hydroxy-blebbistatin, 3'-aminoblebbistatin (47), para-nitroblebbistatin (30), and para-aminoblebbistatin (31), have more favorable properties, like higher water solubility, diminished cytotoxicity, and preserved potency. D-ring-modified BS derivatives with the exception of 3'-hydroxyblebbistatin are non-fluorescent at the spectral range normally used for microscopy or flow cytometry. In the present, study, we investigated the effect of para-nitro- and para-aminoblebbistatin on the growth rate and morphology of neurites in human NPCs. In comparison with blebbistatin, the potency of NBS was similar to that of BS in terms of stimulation of neurite growth, process number, and neurite branching (EC_{50} values are between 2–5 μM). NBS was also slightly more efficacious. However, AmBS was less potent (EC_{50} values are around 10 μM) but more efficacious than BS as regards to neurite growth and branching stimulation. The efficacy of AmBS for promoting new protrusion generation was comparable with that of BS. Human NPCs treated with 80 μM AmBS developed 3–4 (3.67 as an average)

neurites per cell with the total length of 90–100 µm within 3 hours. As an average, every third neurite developed branch in 3 hours.

NMII is regulated by the phosphorylation of its regulatory light chain on Ser19 and Thr18, which is carried out by a number of kinases, including myosin light chain kinase, Rho-associated, coiled coil-containing kinase, leucine-zipper-interacting protein kinase, citron kinase, Serine/Threonine-protein kinase 21, and myotonic dystrophy kinase-related CDC42-binding kinase (25). An equally important part of NMII regulation is its dephosphorylation by phosphatases, such as the myosin light chain phosphatase. The precise cellular localization of these kinases and phosphatases is crucial for the site-specific regulation of NMII, which is necessary to control filopodia dynamics. ROCK is a key component of various converging signaling pathways of upstream Rho-like GTPases. The regulatory role of MLCK and ROCK in neurite outgrowth has been demonstrated by numerous studies based on animal primary neural cell models (4, 7, 12, 16, 19, 48). A recent report, using wild type and RhoA knockout mice as well as primary hippocampal neuron cultures from these animals, suggested a novel mechanism for Rho/ROCK signaling control of the axonal growth, i.e., ROCK restrains protrusion of microtubules to the leading edge of the growth cone by activating NMII-mediated actin arc formation (3). In concert with the animal-based neural models, we found that ROCK1 inhibition similar to blebbistatin promotes neurite outgrowth in human NPCs. Also, their impact on protrusion initialization and process branching were alike. The stimulatory effect of BS and ROCK1 inhibitor was not additive, confirming that ROCK1 is an upstream regulator of NMII also in a human neural model. These results also suggest that ROCK1 signal is manifested mainly by the NMII activity in the regulation of neurite outgrowth. It is worth noting again that previous studies applying animal-based systems investigated the role of NMII in mature neurons, focusing mainly on the growth cone or the axon initial segment, whereas in the present study, we aim at investigating a precursory event, the initialization of neurite formation in neural progenitors.

JNK signaling pathway is two-faced in neural cells by means of promoting either cell development/regeneration or neuronal death/degeneration depending on the cell type, subcellular localization and cellular condition. A JNK1 knockout animal model demonstrated a pivotal role for JNK1 in neuronal microtubule assembly and stabilization (49). Subsequent studies using spiral ganglion or midbrain dopaminergic neurons from rats confirmed the involvement of all three JNK isoforms, although their differential contributions have also been revealed (39, 50). JNK3 was found to be the most prominent in mediating neurite regeneration and cell survival (39). JNK phosphorylation of downstream effectors, such as the dendrite-specific high-molecular-weight microtubule-associated protein 2 (MAP2) and the microtubule-destabilizing protein SCG10, were shown to contribute to defining dendritic architecture and axodendritic length, respectively (51, 52). Contrary to these studies above, which were performed on mature neurons isolated from rodents, Lu et al. employed mouse embryonic neural stem cells (analog of our NPCs) to examine the involvement of JNK (53). Inhibition of JNK diminished valproic acid-induced neurite outgrowth and neuronal differentiation in these cells. In our hands, the specific JNK inhibitor SP600125 did not block either basal neurite outgrowth, or initiation of processes, or branching in human NPCs. Similarly, blocking the JNK pathway did not affect neurite growth elicited by either NMII or ROCK1 inhibition. Several reasons can be accounted for the different effect of JNK inhibition observed in

the previously described cellular models and in our system. Interspecies difference between rodents and humans is one of the plausible explanations. Also, it is known that signaling events greatly dependent on the cell type. NPCs represent an ‘adult’ or more precisely a tissue-specific stem cell population, in which regulatory mechanism can be different from that seen in mature neurons. In addition, as previous studied made it clear, specific cellular localization of kinases in either the RhoA- or the JNK-dependent pathway is crucial for the particular cellular functions (25, 54). It is also noteworthy that we focused only on the initialization, the first 6 hours of neurite generation. Kinetic differences can also be accounted for the conflicting results. Activation of JNK is relatively slow and its kinetics is site-specific in polarized neurons (50). Taken together, we did not see evidence for the involvement of JNK in the regulation of neurite initialization in human NPCs.

Restricted regeneration capability of the central nervous system is determined by both intrinsic and environmental factors. The role of extracellular matrix in neural development and regeneration has long been studied. ECM components in the CNS are produced and secreted by both neurons and glial cells. Some of them, such as laminin and fibronectin, promote neural cell growth and migration, especially in the developing CNS, while others, e.g., chondroitin sulfate proteoglycans, serve as a barrier and prevent axons from growing into improper regions (20). Remodeled ECM constitutes a detrimental environment, imposing a major obstacle for axonal regeneration (21). The effect of these permissive and restrictive ECM components on the neurite outgrowth has been demonstrated *in vitro* using matured neurons (2, 22–24); however, their impact on neural progenitor cells is poorly studied. In the present study, we investigated the neurite outgrowth of human NPCs on various permissive and restrictive ECMs. We found that laminin is an essential component of ECM to accomplish maximal capacity of basal or NBS-stimulated neurite growth. Matrigel was almost as supportive ECM as the laminin-containing coatings. All studied inhibitory ECM components, including aggrecan, CS, MOG, and CSPG, abolished basal neurite outgrowth. Addition of laminin to these inhibitory mixtures reserved the effect of MOG, but only alleviated the constraining effect of the others. However, blebbistatin derivatives, such as NBS and AmBS, were able to override the ECM inhibition in all cases.

Cell therapies using stem cells or stem cell-derived transplants represent a promising and developing field of regenerative medicine. Several stem cell-based preclinical studies and also a limited number of clinical studies have been performed in connection with various CNS pathologies including neurodegenerative disorders [recently reviewed in (55)]. Rodent models of Alzheimer's disease and Huntington's disease showed marked improvement in behavioral and cognitive deficits after transplantation of human iPSC-derived NPCs (56, 57). Similarly, engraftment of human stem cell-derived NPCs or dopaminergic precursors ameliorated bradykinesia and drug-induced rotation behavior in various animal models of Parkinson's disease (58–60). Moreover, early clinical trials have been launched or yet been forthcoming to explore the safety and efficacy of human iPSC-derived progenitors in Parkinson's disease patients [reviewed in (61)]. Functional recovery was also demonstrated in stroke-damaged rodents subjected to human iPSC-derived NPC transplantation (62, 63). The key issue of these interventions is the functional integration of the transplanted cells. Neuronal polarization starting with protrusions of neurites is a prerequisite for NPCs to integrate. However, intrinsic mechanisms and non-permissive nature of CNS

environment for neurite growth greatly impedes this process. Our results demonstrate that targeting NMII can surmount both internal and environmental hindrance of neurite development, offering a new opportunity for improving effectiveness of integration of transplanted cells. Our *in vitro* data can serve as a base for future *in vivo* experiments to explore the potential of pharmacological augmentation of cell therapies for various CNS pathologies.

Conclusions

In summary, we developed an *in vitro* experiment tool for quantitative assessment of neurite outgrowth in human hippocampal dentate gyrus neural progenitors. Using this system, we established the role of NMII in neurite generation, as well as its upstream regulation by the RhoA/ROCK1 signaling pathway. We also demonstrated the effect of permissive and detrimental extracellular matrix components on neurite outgrowth in a human cellular model. Novel, non-toxic derivatives of blebbistatin were found to be highly efficient in stimulating neurite protrusion not only on permissive surfaces but also on ECMs that normally inhibit neurite generation. Thus, our results suggest that NMII and ROCK1 are important pharmacological targets for improving neural regeneration in humans. Revealing the role of NMII in neurite generation of human neural progenitor cells may provide new perspectives in the development of stem cells therapies as NMII might be considered as a novel drug target for integrating transplanted cells in neurodegenerative disorders, such as Parkinson's and Alzheimer's diseases, as well as in traumatic brain and spinal cord injuries (55, 61, 64–67).

Abbreviations

Aggr – aggrecan

AmBS – para-aminoblebbistatin

AU – arbitrary unit

BS – blebbistatin

CNS – central nervous system

CS – chondroitin-sulfate

CSPG – chondroitin-sulfate proteoglycan

EB – embryoid body

ECM – extracellular matrix

eGFP – enhanced green fluorescent protein

eGFP-NPC – enhanced green fluorescent protein-expressing neural progenitor cell

ESC – embryonic stem cell

HUES-NPC – human embryonic stem cell-derived neural progenitor cells

iPSC – induced pluripotent stem cell

iPSC-NPC – induced pluripotent stem cell-derived neural progenitor cells

JNK – c-Jun N-terminal kinase

MAP2 – microtubule-associated protein 2

MOG – myelin oligodendrocyte glycoprotein

NBS – para-nitroblebbistatin

NMII – non-muscle myosin II

NPC – neural progenitor cell

PBS – phosphate-buffered saline

PSC – pluripotent stem cell

ROCK1 – Rho-associated, coiled-coil-containing protein kinase 1

SCG10 – superior cervical ganglion 10

Declarations

Consent and ethical issues

Neither human individuals nor animals were included in this study.

Availability of data and material

The authors declare all data in the manuscript is freely available upon request.

Conflicts of interest/Competing interests

The authors declare no competing interests.

Competing financial interests

A.M-C. is an owner of Motorpharma, Ltd. Motorpharma, Ltd. has a license agreement with Eötvös Loránd University about the development and distribution of para-nitroblebbistatin. The authors declare no other competing financial interests.

Funding

This study has been supported by the National Research, Development and Innovation Office [grant numbers: National Brain Research Program (NAP) 2017-1.2.1-NKP-2017-00002 to L.H., KTIA_NAP_13-2014-0011 to J.M.R., Hungarian Scientific Research Fund (OTKA) K-128123 to L.H., 2019-1.1.1-PIACI-KFI-2019-00488 and TKP2020-IKA-05 to A.M-C.]. The authors also acknowledge the financial support by Szint + Excellence Program of ELTE TTK to A.M-C.

Authors' contributions

Julianna Lilienberg and Zoltán Hegyi (with equal contributions) performed the experiments, analyzed the data, and prepared the original draft. Eszter Szabó and Edit Hathy performed the experiments to generate NPCs stably expressing eGFP. András Málnási-Csizmadia, János M. Réthelyi, and Ágota Apáti contributed to conceptualization and design of the study, as well as to reviewing and editing of the manuscript. László Homolya contributed to study conceptualization and design, supervision of experiments, data analysis, as well as writing and editing of the manuscript. All authors read and approved the final manuscript.

Acknowledgements

The authors thank Beáta Haraszti and Gyöngyi Bézsenyi for technical assistance. The induced pluripotent stem cell (iPSC) line was a kind gift from Fred H. Gage (Salk Institute, USA), while the embryonic stem cell line HUES9 was kindly provided by Douglas Melton (HHMI, USA). Tamás Orbán provided plasmids for enhanced green fluorescent protein (eGFP) delivery. The authors are also grateful to György Várady for cell sorting, as well as to Attila Reményi and Klára Kirsh for testing the c-Jun N-terminal kinase (JNK) inhibitor in an *in vitro* kinase assay. This study has been supported by the National Research, Development and Innovation Office [grant numbers: National Brain Research Program (NAP) 2017-1.2.1-NKP-2017-00002 to L.H., KTIA_NAP_13-2014-0011 to J.M.R., Hungarian Scientific Research Fund (OTKA) K-128123 to L.H., 2019-1.1.1-PIACI-KFI-2019-00488 and TKP2020-IKA-05 to A.M-C]. The authors also acknowledge the financial support by Szint + Excellence Program of ELTE TTK to A.M-C.

References

1. Yu P, Santiago LY, Katagiri Y, Geller HM. Myosin II activity regulates neurite outgrowth and guidance in response to chondroitin sulfate proteoglycans. Journal of neurochemistry. 2012 Mar;120(6):1117-28.
2. Hur EM, Yang IH, Kim DH, Byun J, Saijilafu, Xu WL, et al. Engineering neuronal growth cones to promote axon regeneration over inhibitory molecules. Proceedings of the National Academy of Sciences of the United States of America. 2011 Mar 22;108(12):5057-62.
3. Dupraz S, Hilton BJ, Husch A, Santos TE, Coles CH, Stern S, et al. RhoA Controls Axon Extension Independent of Specification in the Developing Brain. Curr Biol. 2019 Nov 18;29(22):3874-86 e9.

4. Kollins KM, Hu J, Bridgman PC, Huang YQ, Gallo G. Myosin-II negatively regulates minor process extension and the temporal development of neuronal polarity. Dev Neurobiol. 2009 Apr;69(5):279-98.
5. Costa AR, Sousa SC, Pinto-Costa R, Mateus JC, Lopes CD, Costa AC, et al. The membrane periodic skeleton is an actomyosin network that regulates axonal diameter and conduction. Elife. 2020 Mar 20;9.
6. Allingham JS, Smith R, Rayment I. The structural basis of blebbistatin inhibition and specificity for myosin II. Nat Struct Mol Biol. 2005 Apr;12(4):378-9.
7. Kubo T, Endo M, Hata K, Taniguchi J, Kitajo K, Tomura S, et al. Myosin IIA is required for neurite outgrowth inhibition produced by repulsive guidance molecule. Journal of neurochemistry. 2008 Apr;105(1):113-26.
8. Pool M, Rambaldi I, Durafourt BA, Wright MC, Antel JP, Bar-Or A, et al. Myeloid lineage cells inhibit neurite outgrowth through a myosin II-dependent mechanism. J Neuroimmunol. 2011 Aug 15;237(1-2):101-5.
9. Spedden E, Wiens MR, Demirel MC, Staii C. Effects of surface asymmetry on neuronal growth. PLoS One. 2014;9(9):e106709.
10. Roland AB, Ricobaraza A, Carrel D, Jordan BM, Rico F, Simon A, et al. Cannabinoid-induced actomyosin contractility shapes neuronal morphology and growth. Elife. 2014 Sep 15;3:e03159.
11. Evans MD, Tufo C, Dumitrescu AS, Grubb MS. Myosin II activity is required for structural plasticity at the axon initial segment. Eur J Neurosci. 2017 Jul;46(2):1751-7.
12. Wang Y, Xu Y, Liu Q, Zhang Y, Gao Z, Yin M, et al. Myosin IIA-related Actomyosin Contractility Mediates Oxidative Stress-induced Neuronal Apoptosis. Frontiers in molecular neuroscience. 2017;10:75.
13. Tanaka A, Fujii Y, Kasai N, Okajima T, Nakashima H. Regulation of neuritogenesis in hippocampal neurons using stiffness of extracellular microenvironment. PLoS One. 2018;13(2):e0191928.
14. Basso JMV, Yurchenko I, Wiens MR, Staii C. Neuron dynamics on directional surfaces. Soft Matter. 2019 Dec 11;15(48):9931-41.
15. Wang T, Li W, Martin S, Papadopulos A, Joensuu M, Liu C, et al. Radial contractility of actomyosin rings facilitates axonal trafficking and structural stability. J Cell Biol. 2020 May 4;219(5).
16. Rosner H, Moller W, Wassermann T, Mihatsch J, Blum M. Attenuation of actinomyosinII contractile activity in growth cones accelerates filopodia-guided and microtubule-based neurite elongation. Brain Res. 2007 Oct 24;1176:1-10.
17. Xie J, Liu W, MacEwan MR, Bridgman PC, Xia Y. Neurite outgrowth on electrospun nanofibers with uniaxial alignment: the effects of fiber density, surface coating, and supporting substrate. ACS Nano. 2014 Feb 25;8(2):1878-85.
18. Medeiros NA, Burnette DT, Forscher P. Myosin II functions in actin-bundle turnover in neuronal growth cones. Nat Cell Biol. 2006 Mar;8(3):215-26.

19. Tornieri K, Welshhans K, Geddis MS, Rehder V. Control of neurite outgrowth and growth cone motility by phosphatidylinositol-3-kinase. Cell Motil Cytoskeleton. 2006 Apr;63(4):173-92.
20. Baldwin KT, Giger RJ. Insights into the physiological role of CNS regeneration inhibitors. Frontiers in molecular neuroscience. 2015;8:23.
21. Beller JA, Snow DM. Proteoglycans: road signs for neurite outgrowth. Neural regeneration research. 2014 Feb 15;9(4):343-55.
22. Ichikawa N, Iwabuchi K, Kurihara H, Ishii K, Kobayashi T, Sasaki T, et al. Binding of laminin-1 to monosialoganglioside GM1 in lipid rafts is crucial for neurite outgrowth. J Cell Sci. 2009 Jan 15;122(Pt 2):289-99.
23. Tan CL, Kwok JC, Patani R, Ffrench-Constant C, Chandran S, Fawcett JW. Integrin activation promotes axon growth on inhibitory chondroitin sulfate proteoglycans by enhancing integrin signaling. J Neurosci. 2011 Apr 27;31(17):6289-95.
24. Nakamura A, Morise J, Yabuno-Nakagawa K, Hashimoto Y, Takematsu H, Oka S. Site-specific HNK-1 epitope on alternatively spliced fibronectin type-III repeats in tenascin-C promotes neurite outgrowth of hippocampal neurons through contactin-1. PLoS One. 2019;14(1):e0210193.
25. Costa AR, Sousa MM. Non-Muscle Myosin II in Axonal Cell Biology: From the Growth Cone to the Axon Initial Segment. Cells. 2020 Aug 26;9(9).
26. Straight AF, Cheung A, Limouze J, Chen I, Westwood NJ, Sellers JR, et al. Dissecting temporal and spatial control of cytokinesis with a myosin II Inhibitor. Science. 2003 Mar 14;299(5613):1743-7.
27. Kovacs M, Toth J, Hetenyi C, Malnasi-Csizmadia A, Sellers JR. Mechanism of blebbistatin inhibition of myosin II. The Journal of biological chemistry. 2004 Aug 20;279(34):35557-63.
28. Zhao CS, Overstreet-Wadiche L. Integration of adult generated neurons during epileptogenesis. Epilepsia. 2008 Jun;49 Suppl 5:3-12.
29. Roman BI, Verhasselt S, Stevens CV. Medicinal Chemistry and Use of Myosin II Inhibitor (S)-Blebbistatin and Its Derivatives. J Med Chem. 2018 Nov 8;61(21):9410-28.
30. Kepiro M, Varkuti BH, Vegner L, Voros G, Hegyi G, Varga M, et al. para-Nitroblebbistatin, the non-cytotoxic and photostable myosin II inhibitor. Angewandte Chemie. 2014 Jul 28;53(31):8211-5.
31. Varkuti BH, Kepiro M, Horvath IA, Vegner L, Rati S, Zsigmond A, et al. A highly soluble, non-phototoxic, non-fluorescent blebbistatin derivative. Scientific reports. 2016 May 31;6:26141.
32. Rauscher AA, Gyimesi M, Kovacs M, Malnasi-Csizmadia A. Targeting Myosin by Blebbistatin Derivatives: Optimization and Pharmacological Potential. Trends Biochem Sci. 2018 Sep;43(9):700-13.
33. Gyimesi M, Rauscher AA, Suthar SK, Hamow KA, Oravecz K, Lorincz I, et al. Improved Inhibitory and Absorption, Distribution, Metabolism, Excretion, and Toxicology (ADMET) Properties of Blebbistatin Derivatives Indicate That Blebbistatin Scaffold Is Ideal for drug Development Targeting Myosin-2. J Pharmacol Exp Ther. 2021 Mar;376(3):358-73.

34. Vofely G, Berecz T, Szabo E, Szebenyi K, Hathy E, Orban TI, et al. Characterization of calcium signals in human induced pluripotent stem cell-derived dentate gyrus neuronal progenitors and mature neurons, stably expressing an advanced calcium indicator protein. Molecular and cellular neurosciences. 2018 Apr;88:222-30.
35. Yu DX, Di Giorgio FP, Yao J, Marchetto MC, Brennand K, Wright R, et al. Modeling hippocampal neurogenesis using human pluripotent stem cells. Stem cell reports. 2014 Mar 11;2(3):295-310.
36. Kolacsek O, Erdei Z, Apati A, Sandor S, Izsvak Z, Ivics Z, et al. Excision efficiency is not strongly coupled to transgenic rate: cell type-dependent transposition efficiency of sleeping beauty and piggyBac DNA transposons. Hum Gene Ther Methods. 2014 Aug;25(4):241-52.
37. Turney SG, Bridgman PC. Laminin stimulates and guides axonal outgrowth via growth cone myosin II activity. Nat Neurosci. 2005 Jun;8(6):717-9.
38. Zhang XF, Schaefer AW, Burnette DT, Schoonderwoert VT, Forscher P. Rho-dependent contractile responses in the neuronal growth cone are independent of classical peripheral retrograde actin flow. Neuron. 2003 Dec 4;40(5):931-44.
39. Tonges L, Planchamp V, Koch JC, Herdegen T, Bahr M, Lingor P. JNK isoforms differentially regulate neurite growth and regeneration in dopaminergic neurons in vitro. Journal of molecular neuroscience : MN. 2011 Oct;45(2):284-93.
40. Lowery LA, Van Vactor D. The trip of the tip: understanding the growth cone machinery. Nature reviews Molecular cell biology. 2009 May;10(5):332-43.
41. Eggert US, Mitchison TJ, Field CM. Animal cytokinesis: from parts list to mechanisms. Annual review of biochemistry. 2006;75:543-66.
42. Vicente-Manzanares M, Ma X, Adelstein RS, Horwitz AR. Non-muscle myosin II takes centre stage in cell adhesion and migration. Nature reviews Molecular cell biology. 2009 Nov;10(11):778-90.
43. Ankam S, Lim CK, Yim EK. Actomyosin contractility plays a role in MAP2 expression during nanotopography-directed neuronal differentiation of human embryonic stem cells. Biomaterials. 2015 Apr;47:20-8.
44. Xue Y, Zhan X, Sun S, Karuppagounder SS, Xia S, Dawson VL, et al. Synthetic mRNAs Drive Highly Efficient iPS Cell Differentiation to Dopaminergic Neurons. Stem Cells Transl Med. 2019 Feb;8(2):112-23.
45. Sherman SP, Bang AG. High-throughput screen for compounds that modulate neurite growth of human induced pluripotent stem cell-derived neurons. Dis Model Mech. 2018 Feb 2;11(2).
46. Verhasselt S, Stevens CV, Van den Broecke T, Bracke ME, Roman BI. Insights into the myosin II inhibitory potency of A-ring-modified (S)-blebbistatin analogs. Bioorg Med Chem Lett. 2017 Jul 1;27(13):2986-9.
47. Verhasselt S, Roman BI, De Wever O, Van Hecke K, Van Deun R, Bracke ME, et al. Discovery of (S)-3'-hydroxyblebbistatin and (S)-3'-aminoblebbistatin: polar myosin II inhibitors with superior research tool properties. Org Biomol Chem. 2017 Mar 1;15(9):2104-18.

48. Al-Ali H, Lee DH, Danzi MC, Nassif H, Gautam P, Wennerberg K, et al. Rational Polypharmacology: Systematically Identifying and Engaging Multiple Drug Targets To Promote Axon Growth. ACS Chem Biol. 2015 Aug 21;10(8):1939-51.
49. Chang L, Jones Y, Ellisman MH, Goldstein LS, Karin M. JNK1 is required for maintenance of neuronal microtubules and controls phosphorylation of microtubule-associated proteins. Dev Cell. 2003 Apr;4(4):521-33.
50. Atkinson PJ, Cho CH, Hansen MR, Green SH. Activity of all JNK isoforms contributes to neurite growth in spiral ganglion neurons. Hear Res. 2011 Aug;278(1-2):77-85.
51. Bjorkblom B, Ostman N, Hongisto V, Komarovski V, Filen JJ, Nyman TA, et al. Constitutively active cytoplasmic c-Jun N-terminal kinase 1 is a dominant regulator of dendritic architecture: role of microtubule-associated protein 2 as an effector. J Neurosci. 2005 Jul 6;25(27):6350-61.
52. Tararuk T, Ostman N, Li W, Bjorkblom B, Padzik A, Zdrojewska J, et al. JNK1 phosphorylation of SCG10 determines microtubule dynamics and axodendritic length. J Cell Biol. 2006 Apr 24;173(2):265-77.
53. Lu L, Zhou H, Pan B, Li X, Fu Z, Liu J, et al. c-Jun Amino-Terminal Kinase is Involved in Valproic Acid-Mediated Neuronal Differentiation of Mouse Embryonic NSCs and Neurite Outgrowth of NSC-Derived Neurons. Neurochem Res. 2017 Apr;42(4):1254-66.
54. Coffey ET. Nuclear and cytosolic JNK signalling in neurons. Nat Rev Neurosci. 2014 May;15(5):285-99.
55. Ford E, Pearlman J, Ruan T, Manion J, Waller M, Neely GG, et al. Human Pluripotent Stem Cells-Based Therapies for Neurodegenerative Diseases: Current Status and Challenges. Cells. 2020 Nov 20;9(11).
56. Fujiwara N, Shimizu J, Takai K, Arimitsu N, Saito A, Kono T, et al. Restoration of spatial memory dysfunction of human APP transgenic mice by transplantation of neuronal precursors derived from human iPS cells. Neurosci Lett. 2013 Dec 17;557 Pt B:129-34.
57. Jeon I, Choi C, Lee N, Im W, Kim M, Oh SH, et al. In Vivo Roles of a Patient-Derived Induced Pluripotent Stem Cell Line (HD72-iPSC) in the YAC128 Model of Huntington's Disease. Int J Stem Cells. 2014 May;7(1):43-7.
58. Han F, Wang W, Chen B, Chen C, Li S, Lu X, et al. Human induced pluripotent stem cell-derived neurons improve motor asymmetry in a 6-hydroxydopamine-induced rat model of Parkinson's disease. Cytotherapy. 2015 May;17(5):665-79.
59. Roy NS, Cleren C, Singh SK, Yang L, Beal MF, Goldman SA. Functional engraftment of human ES cell-derived dopaminergic neurons enriched by coculture with telomerase-immortalized midbrain astrocytes. Nat Med. 2006 Nov;12(11):1259-68.
60. Kriks S, Shim JW, Piao J, Ganat YM, Wakeman DR, Xie Z, et al. Dopamine neurons derived from human ES cells efficiently engraft in animal models of Parkinson's disease. Nature. 2011 Nov 6;480(7378):547-51.
61. Parmar M, Grealish S, Henchcliffe C. The future of stem cell therapies for Parkinson disease. Nat Rev Neurosci. 2020 Feb;21(2):103-15.

62. Gomi M, Takagi Y, Morizane A, Doi D, Nishimura M, Miyamoto S, et al. Functional recovery of the murine brain ischemia model using human induced pluripotent stem cell-derived telencephalic progenitors. Brain Res. 2012 Jun 12;1459:52-60.
63. Mohamad O, Drury-Stewart D, Song M, Faulkner B, Chen D, Yu SP, et al. Vector-free and transgene-free human iPS cells differentiate into functional neurons and enhance functional recovery after ischemic stroke in mice. PLoS One. 2013;8(5):e64160.
64. Bagheri-Mohammadi S. Stem cell-based therapy as a promising approach in Alzheimer's disease: current perspectives on novel treatment. Cell Tissue Bank. 2021 Jan 4.
65. Liu XY, Yang LP, Zhao L. Stem cell therapy for Alzheimer's disease. World J Stem Cells. 2020 Aug 26;12(8):787-802.
66. Hu XC, Lu YB, Yang YN, Kang XW, Wang YG, Ma B, et al. Progress in clinical trials of cell transplantation for the treatment of spinal cord injury: how many questions remain unanswered? Neural regeneration research. 2021 Mar;16(3):405-13.
67. Lengel D, Sevilla C, Romm ZL, Huh JW, Raghupathi R. Stem Cell Therapy for Pediatric Traumatic Brain Injury. Front Neurol. 2020;11:601286.

Figures

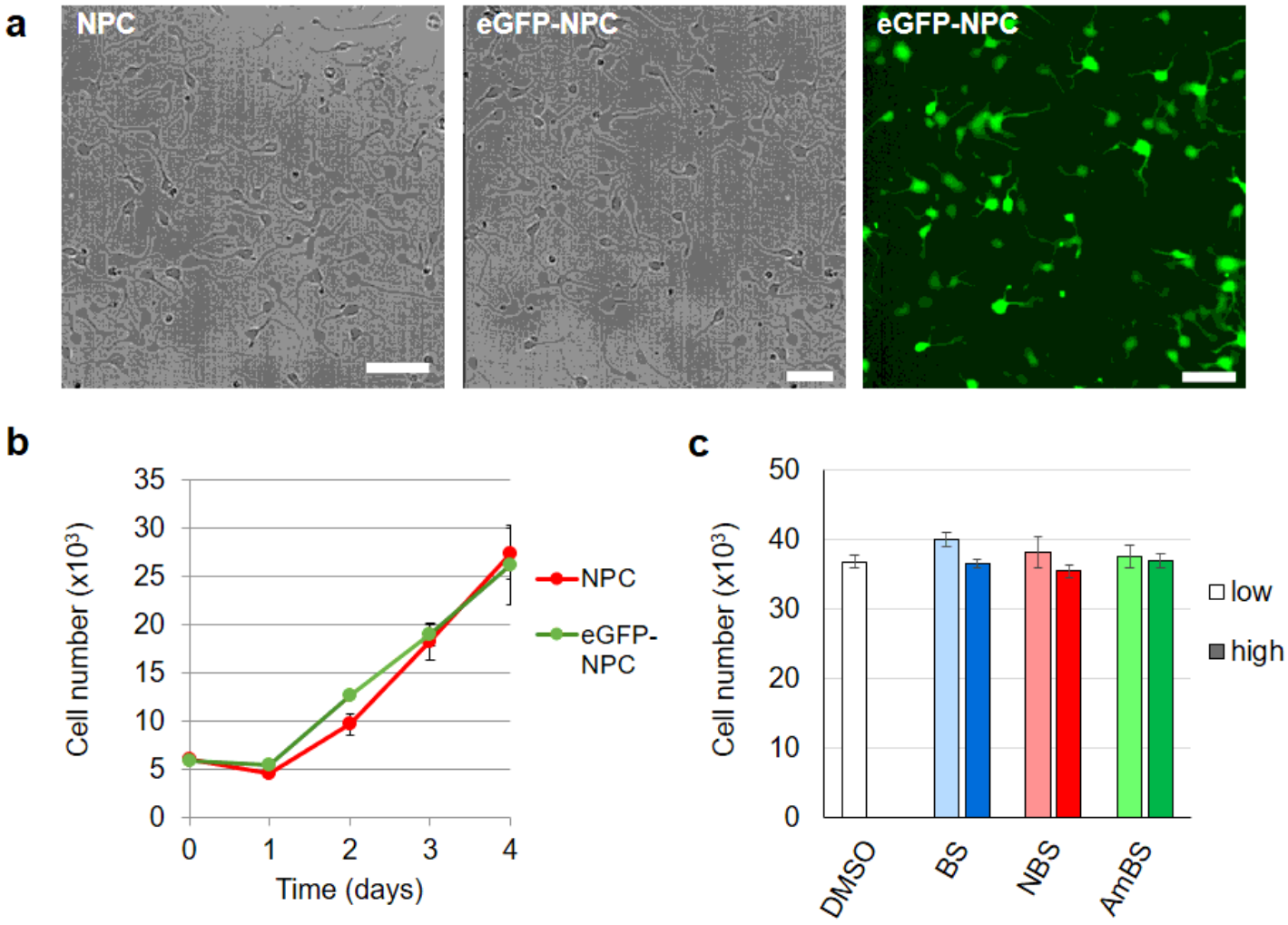

Figure 1

Characterization of human neural progenitor cells stably expressing eGFP eGFF was stably expressed in human NPCs using a Sleeping Beauty transposon-based expression system. (a) No morphological difference between the parental (NPC) and the GFP-expressing NPCs (eGFP-NPC) can be observed. However, the transfectants exhibit uniform green fluorescence, making not only the cell body but also the neurites visible. (b) There is no difference in the proliferation capacity of NPCs and eGFP-NPCs. (c) The cytotoxic effects of blebbistatin (BS), para-nitroblebbistatin (NBS), and para-aminoblebbistatin (AmBS) was investigated by subjecting eGFP-NPCs (3 x 104) to these compounds 2 hours after seeding. BS and NBS were applied at 10 or 20 μM concentrations marked as low and high, respectively; whereas AmBS was used at 20 or 40 μM concentrations. The cell numbers were determined 4 hours after the treatments and compared to the cell number of the vehicle (DMSO) treated sample. The mean ± SEM values from three independent experiments are shown in Panels B and C. No significant differences were found.

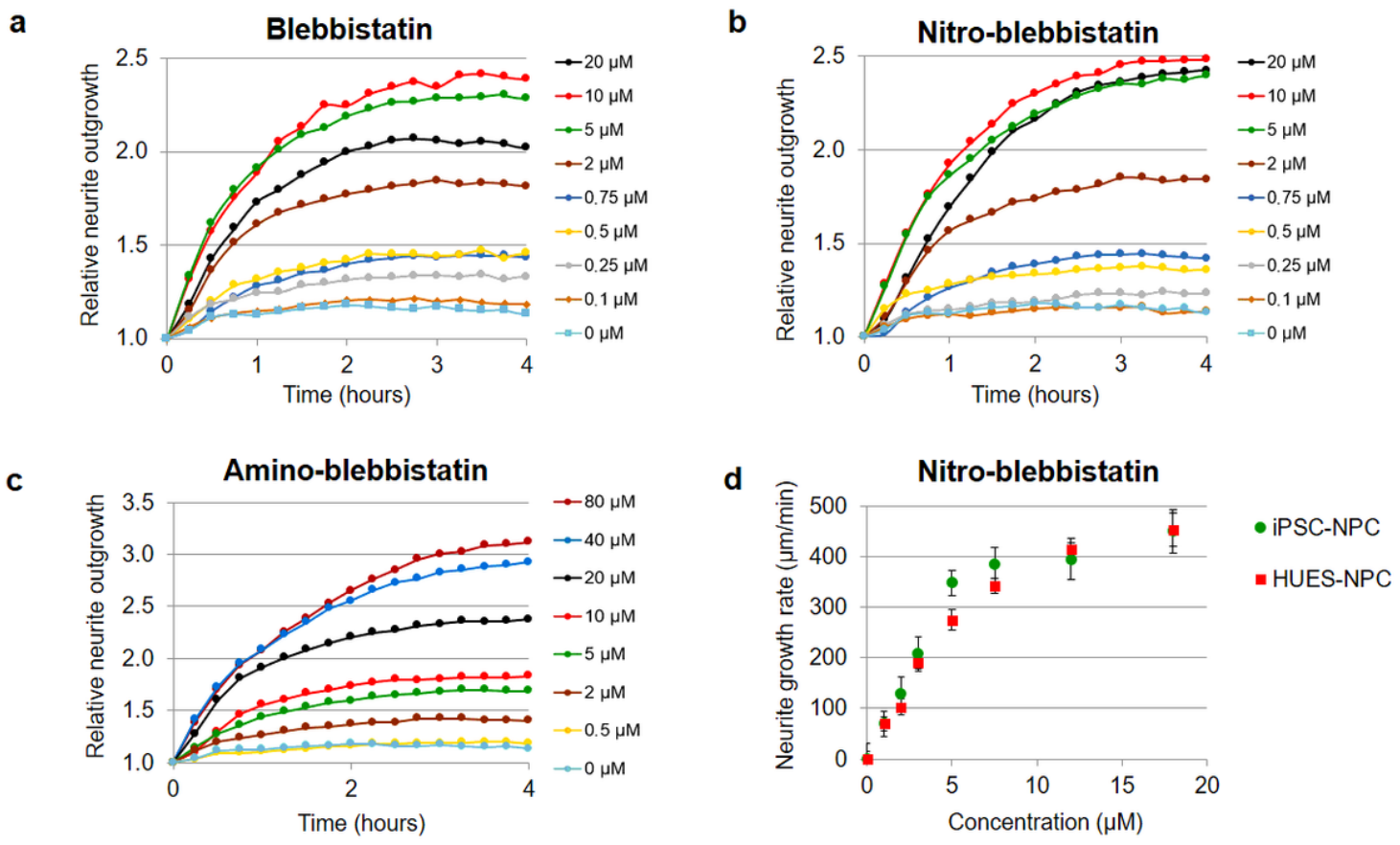

Figure 2

Effect of blebbistatin and blebbistatin derivatives on the neurite outgrowth of NPCs (a-c) NPCs stably expressing eGFP were subjected to blebbistatin, para-nitroblebbistatin, or para-aminoblebbistatin in the indicated concentrations. The total lengths of neurites were determined in six fields of view containing 120-150 cells each. The neurite lengths were normalized to the initial values. All three compounds stimulated neurite outgrowth in a dose dependent manner. The EC50 values for BS and NBS were about 2 μM, whereas that for AmBS was above 10 μM. Panels A-C depict representative experiments. (d) Dose-response curves for NBS-stimulated neurite outgrowth analyzed in two human NPCs with different origin, i.e., iPSC-derived neural progenitor cells (iPSC-NPC) and NPCs differentiated from the human embryonic stem cell line HUES9 (HUES-NPC). Both NPC lines stably expressed eGFP. The neurite outgrowth rates were determined from the initial growth rates. The mean ± SEM values from three independent experiments are shown. No marked difference was observed between the two cell lines.

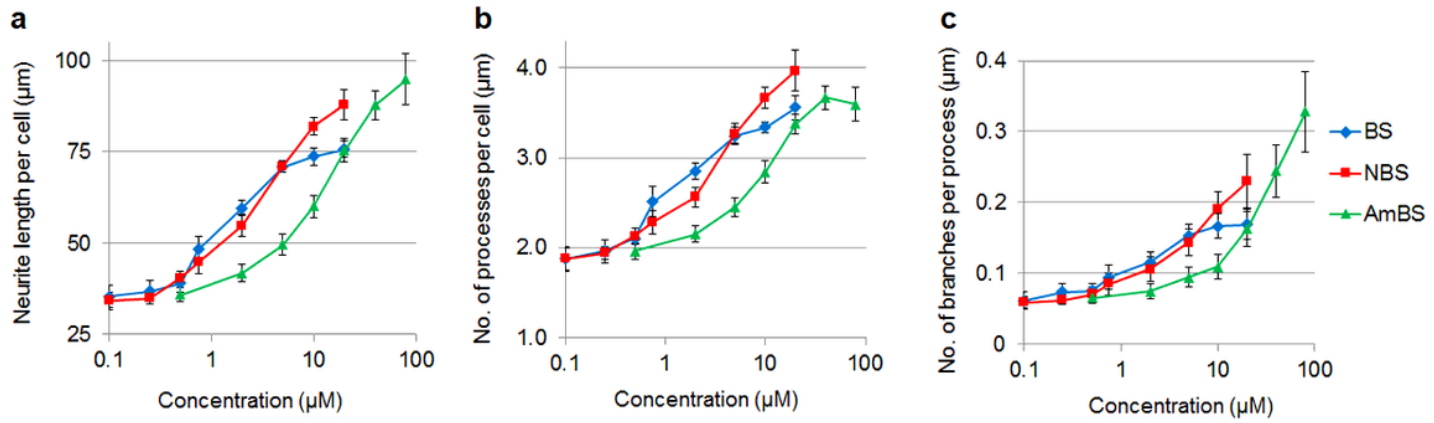

Figure 3

Dose response curves for various morphological parameters of NPCs treated with blebbistatin or blebbistatin derivatives BS, NBS, and AmBS increased the neurite length per cell (a), elevated the number of projections per cell (b), and stimulated neurite branching (c) in dose dependent manners. The values were determined three hours after treatment. The mean ± SEM from three independent experiments are indicated.

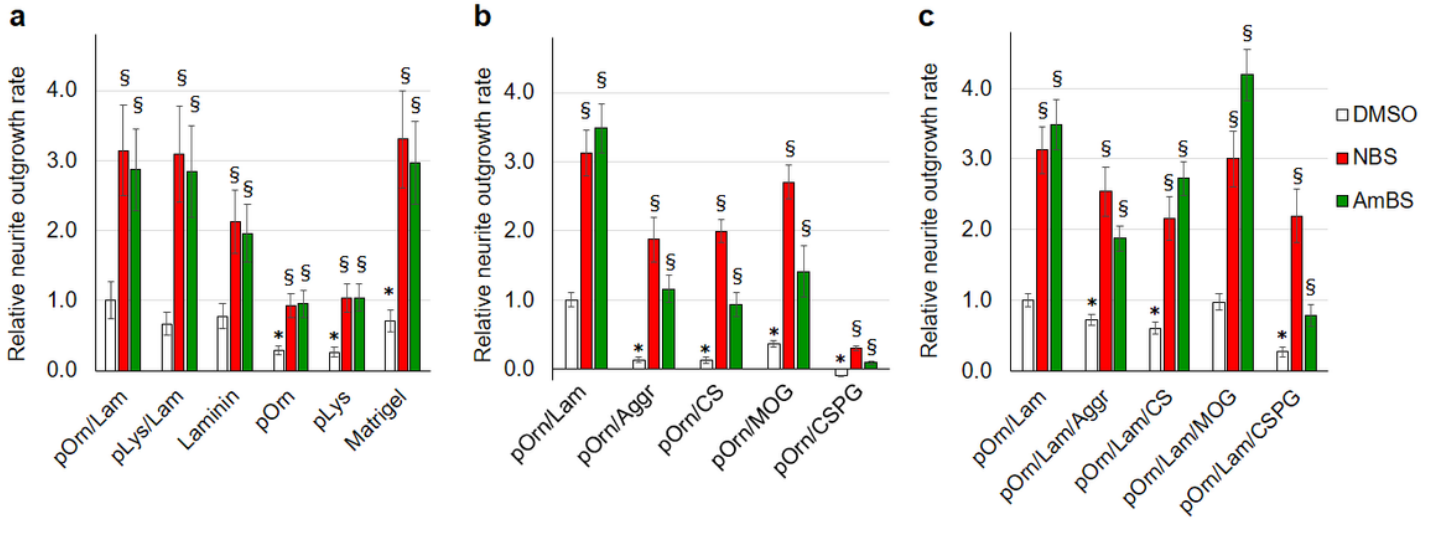

Figure 4

Effect of various extracellular matrices on the neurite outgrowth (a) Human NPCs were seeded onto culturing plates coated with permissive ECM components, such as laminin, poly-ornithine (pOrn), poly-lysine (pLys), Matrigel, the combination of poly-ornithine and laminin (pOrn/Lam), or the combination of poly-lysine and laminin (pLys/Lam). Neurite outgrowth was monitored in the presence and absence of

para-nitroblebbistatin (10 μM) or para-aminoblebbistatin (20 μM). The neurite outgrowth rates were determined from the initial growth rates. The neurite outgrowth rate measured in cells seeded onto pOrn/Lam-coated surface was used as a reference point, and all growth rates were normalized to this value. (b) Neurite outgrowth rates were determined in NPCs plated onto coatings containing poly-ornithine (pOrn) in combination with restrictive ECM components, including aggrecan (Aggr), chondroitin sulfate (CS), myelin oligodendrocyte glycoprotein (MOG), or chondroitin sulfate proteoglycan (CSPG). As a reference point, the neurite outgrowth rate of cells on pOrn/Lam-coated surface was used. All four ECM components inhibited neurite outgrowth of NPCs. When the cells were treated with NBS or AmBS extensive neurite outgrowth was observed except for the cells seeded onto pOrn/CSPG-coated surface. (c) An experiment similar to that shown in Panel B was performed with the difference that laminin was also included in the coatings. In this combination, MOG was not detrimental to the cells, and BS derivatives were able to override the inhibitory effect of not only Aggr, CS, and MOG, but also of CSPG. In all panels, the mean ± SEM from at least three independent experiments are indicated. Asterisks and section signs indicate significant differences as compared to the samples grown on pOrn/Lam-coated surface and to those were not treated with BS derivatives (white columns), respectively ($p < 0.05$).

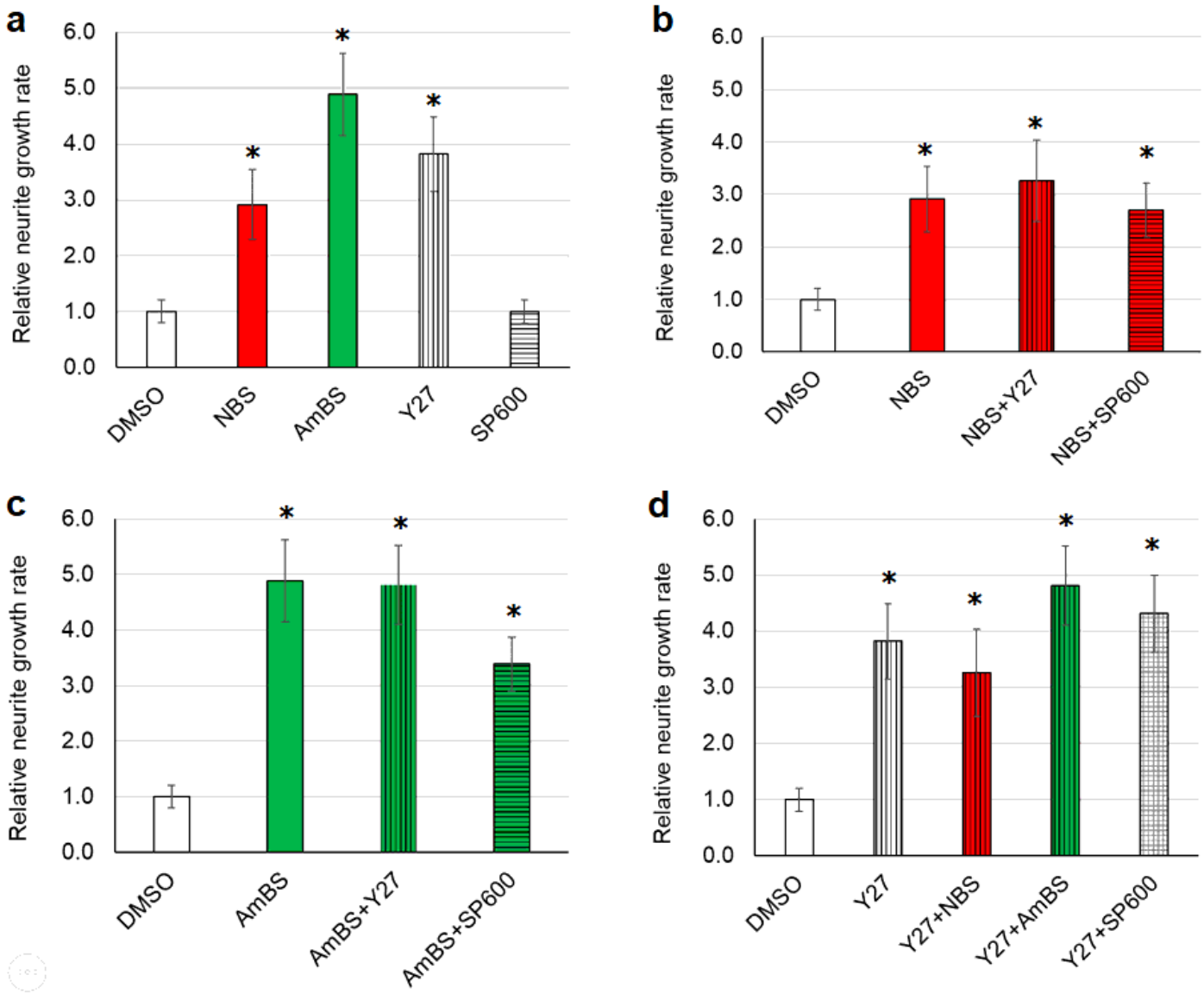

Figure 5

Effect of potential upstream regulators on basal and BS derivative-stimulated neurite outgrowth a) NPCs were subjected to the ROCK1 inhibitor, Y27632 (10 μM) or the JNK inhibitor, SP600125 (10 μM), and the neurite outgrowth was monitored. The outgrowth rates were determined from the initial rates and normalized to the DMSO (vehicle) control. Stimulations by NBS and AmBS were used as reference points. The ROCK1 inhibitor stimulated neurite outgrowth to similar extent to that seen with NBS and AmBS. In contrast, JNK inhibition had no effect on neurite outgrowth in human NPCs. (b) When the Y27632 or SP600125 was co-administered with NBS, neither additivity nor inhibition was seen. (c) Similar results were obtained with AmBS. (d) Similar to NBS and AmBS, SP600125 did not alter Y27632-stimulated neurite outgrowth. All panels depict the means ± SEM from 3-5 independent experiments. Asterisks indicate significant differences as compared to the DMSO control ($p < 0.05$).

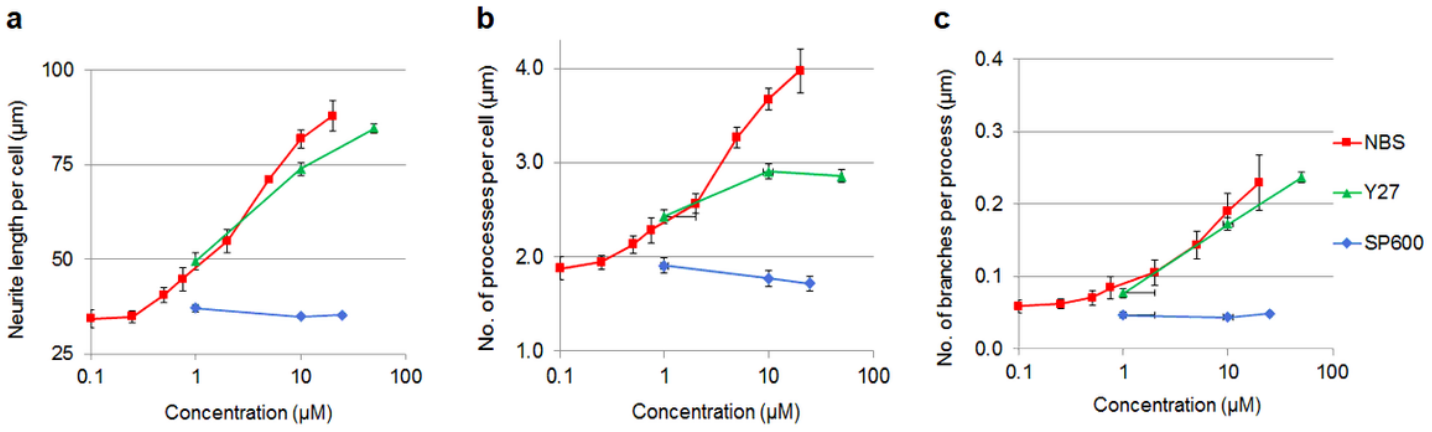

Figure 6

Dose response curves for various morphological parameters of NPCs treated with ROCK1 and JNK inhibitors The neurite length per cell (a), the number of projections per cell (b), as well as the neurite branching (c) was stimulated by Y27632 in dose dependent manners, whereas SP600125 had no such effects. The values were determined three hours after treatment. The NBS stimulated dose response curves were used as references. The mean ± SEM from three independent experiments are shown.

Supplementary Files

This is a list of supplementary files associated with this preprint. Click to download.

- Supplementary1.tif
- Supplementary2.tif
- Supplementary3.tif
- Supplementary4.tif

- SupplementaryVideo1.avi
- SupplementaryVideo2.avi